Theor Chem Account (2008) 120:551–556
DOI 10.1007/s00214-008-0425-8

REGULAR ARTICLE

Ab initio modeling of TiO_2 nanosheets

Andrea Vittadini · Maurizio Casarin

Received: 2 November 2007 / Accepted: 8 February 2008 / Published online: 29 February 2008

Abstract We present density functional calculations on 1–6 monolayer (ML) thick TiO_2 films peeled off from the main low-index surfaces of anatase. The structure of the films is optimized both by constraining the lattice constants to those of bulk anatase, and by allowing them to relax. It is found that the stability order of the films does not follow that of the surfaces from which they are derived, and does not increase monotonously with film thickness. Furthermore, relaxing the lattice constants can induce large modifications in the film structure. In particular, two anomalously stable films are found. One derives from the 2 ML (001) film, and rearranges to a lepidocrocite-TiO_2 nanosheet. The other one derives from a 4 ML (101) film, and gives rise to a novel phase, where all the Ti ions are fivefold coordinated.

Keywords Titanium dioxide · Nanosheets · Density functional calculations

1 Introduction

Titania (TiO_2) is one of the most versatile metal oxides, as is it widely adopted in heterogenous catalysis, photocatalysis, and photovoltaics applications [1–3]. Because the most active polymorph, anatase, is not stable as a bulk phase [4], TiO_2 is commonly used under the form of nanosized particles since decades. Recently, the need of obtaining a better control in the size and the shape of metal oxide nanoparticles has been boosted by the search for materials of improved performance. This has stimulated both work in the field of synthesis [5,6] as well as investigations on model systems in UHV [7,8]. Particular interest is being devoted to TiO_2 nanosheets, which are two-dimensional systems having a thickness of a few atomic layers. In spite of their low dimensionality, TiO_2 nanosheets can be remarkably stable. In particular, lepidocrocite structured nanosheets, where Ti ions are in a sixfold coordinated configuration, were computed to be only 0.18 eV/unit formula higher in energy with respect to bulk TiO_2[9]. This has suggested the use of lepidocrocite TiO_2 as a building block for complex nanostructured materials, as multilayer and composite systems [10–13]. Furthermore, lepidocrocite nanosheets can be possibly wrapped up in nanotubes, even though this issue is still debated [14–28]. An interesting feature of lepidocrocite TiO_2 layers is their close structural relationship with anatase. In fact, recent density functional theory (DFT) investigations showed that a bilayer of (001)-oriented TiO_2-anatase can be converted through a barrierless pathway into a lepidocrocite nanosheet, by allowing the upper half of the bilayer slide over the lower half [7]. A similar conclusion has been obtained by molecular dynamics (MD) investigations on 1D periodic models cut out from (001)-oriented TiO_2-anatase slabs [29]. It is known that on decreasing the cystallite size, the favored titania phase turns out to be the thermodynamically unstable anatase one, because of its low surface energy [4,30,31]. However, the instability of thin anatase TiO_2 layers with respect to lepidocrocite nanosheeets shows that on reducing one or more particle dimensions to subnanoscopic size, other structures may be stable. In this work we perform a systematic investigation of the energetics of structures obtained by peeling off ultrathin layers from low-index surfaces of anatase TiO_2, with the aim of verifying whether stable TiO_2 nanolayers with structure other than lepidocrocite exist.

Contribution to the Nino Russo Special Issue.

A. Vittadini (✉) · M. Casarin
ISTM-CNR, Dipartimento di Scienze Chimiche (DSC),
Università di Padova, via Marzolo 1, 35131 Padova, Italy
e-mail: andrea.vittadini@unipd.it

2 Computational details

We considered anatase TiO_2 thin films of thickness ranging from 1 to 6 monolayers (ML), which were modeled with slabs repeated along the z direction. We considered the main low-index surfaces of anatase (Fig. 1). We adopted a plane-wave basis set, Vanderbilt ultrasoft pseudopotentials [32] and the Perdew–Burke–Ernzerhof [33] exchange-correlation functional. Valence states include 2s and 2p shells for O (six electrons), and 3s, 3p, 3d, and 4s states for Ti (12 valence electrons). Consecutive slabs were separated by a vacuum region of at least 10 Å. Both the internal and the lattice constants of the slab models were optimized. The configuration space was first explored by computing total energies over coarse grids where the film constants were elongated/contracted up to ±25% wrt the bulk values. Minima structures were refined by variable-cell runs using a Wentzcovitch damped dynamics [34]. Test carried out on bulk TiO_2 showed that results of converged fixed-cutoff calculations are reproduced by variable-cell calculations with a kinetic-energy cutoff of 50 Ry for the wavefunctions, and of 400 Ry for the augmentation charge. We emphasize that, though we optimized the film structures thoroughly (no symmetry was considered during the optimization runs) the aim of our work was not that of obtaining the global minimum starting from a given distributions of cations and anions, but rather that of exploring the architectures of possible TiO_2 nanolayers whose structure is connected to that of anatase. To compare the energy of different films, we define a formation energy per TiO_2 unit (E_{film}) as follows:

$$E_{\mathrm{film}} = E_{\mathrm{tot}}(\mathrm{slab})/n - E_{\mathrm{tot}}(\mathrm{TiO_2}) \quad (1)$$

where $E_{\mathrm{tot}}(\mathrm{slab})$ is the total energy of the slab model, $E_{\mathrm{tot}}(\mathrm{TiO_2})$ is the total energy of bulk anatase per unit formula, and n is the number stoichiometric TiO_2 units forming the slab unit cell. We indicate as E_{film} and E'_{film} values computed *before* and *after* allowing the slab constants to relax, respectively (ion positions were fully relaxed in both cases). For films whose lateral size was constrained to the bulk lattice constants, we can also define a surface energy which can be compared to that of the surface from which they were peeled off. This energy (E_{surf}) is also reported, and was computed as:

$$E_{\mathrm{surf}} = [E_{\mathrm{tot}}(\mathrm{slab}) - n \times E_{\mathrm{tot}}(\mathrm{TiO_2})]/2A \quad (2)$$

where A is the area of the film surface.

3 Results and discussion

(001)-oriented films. The (001) surface has a square unit cell, and is characterized by the presence of rows of two-fold coordinated anions (O_{2c}). Each O_{2c} ion in the unrelaxed structure is symmetrically connected to two fivefold coordinated cations (Ti_{5c}), which yields –Ti_{5c}–O_{2c}– chains running perpendicular to the O_{2c} rows. Relaxation schemes of metal oxide surfaces usually involve the shortening of the bonds between undercoordinated ions, while cations and anions move inward and outward, respectively. However, in the case of the anatase (001) surface these stabilization criteria are conflicting. This drives a symmetry breaking of the surface chains, which are converted in a sequence of alternating short (double) and long (dative) Ti_{5c}–O_{2c} bonds [30,31]. Even when relaxed, the surface is however under tensile stress, which can be put in relation with the unnatural bond angle at the O_{2c} ions (∼150°). This explains why on annealed samples the (001) surface is (1 × 4)-reconstructed. Theoretical calculations by Lazzeri and Selloni [35] indicate that this corresponds to a structure where one out of four

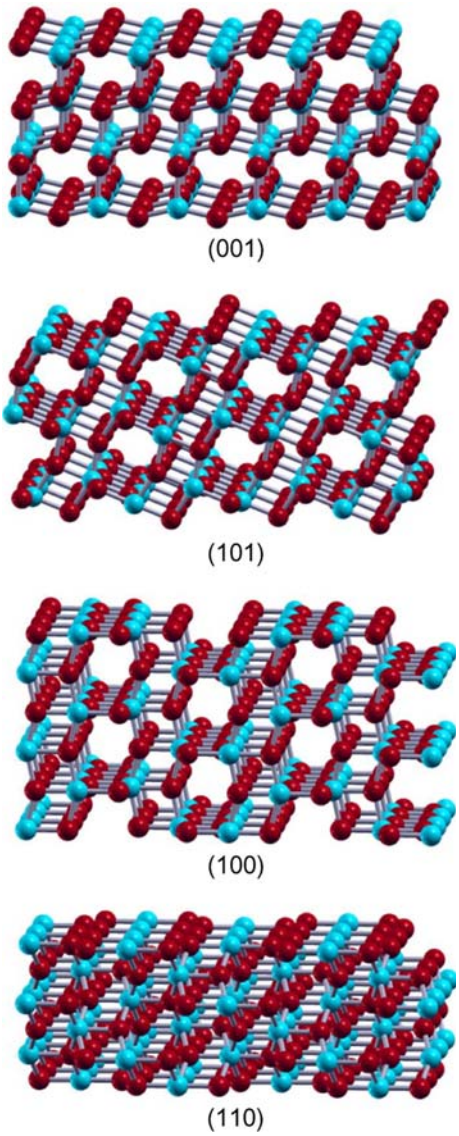

Fig. 1 Ball-and-sticks models of most stable low-index anatase surfaces

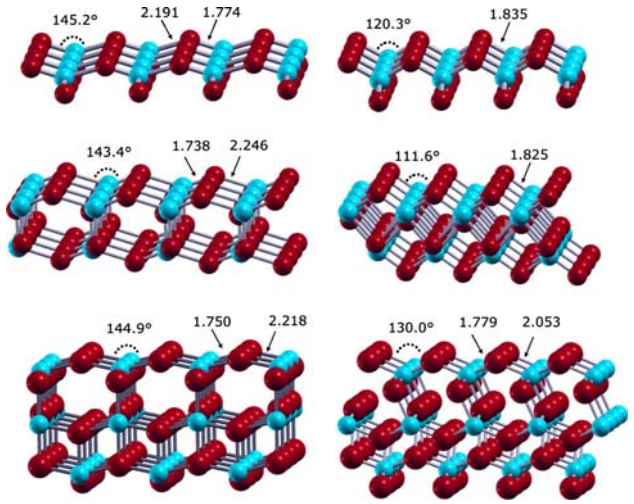

Fig. 2 From *top* to *bottom*: relaxed structures of 1 ML, 2 ML, and 3 ML (001)-oriented films. Structures on the *left* (*right*) are those obtained with bulk (optimized) constants. Displayed bond lengths are in Å

Table 1 Structural and energy parameters of TiO_2 films derived from the (001) anatase surface, and consisting of a number layers $1 \leq N_{lay} \leq 6$

N_{lay}	E_{film}	E_{surf}	a'	b'	E'_{film}
1	2.09	1.17	3.185	3.185	0.65
2	0.78	0.87	3.730	3.020	0.16
3	0.53	0.90	3.575	3.475	0.44
4	0.41	0.91	3.863	3.407	0.24
5	0.32	0.91	3.716	3.716	0.31
6	0.27	0.90	3.862	3.520	0.21

E_{film} (in eV/TiO_2) is the film energy wrt bulk anatase, while E_{surf} (in J/m^2) is the surface energy. Both values are computed by constraining the film constants to those of bulk anatase ($a = 3.786$ Å, $b = 3.786$ Å). E'_{film} is the film energy computed for the a' and b' optimized constants

O_{2c} rows are replaced by a "polymer" of TiO_3 stoichiometry which are characterized by a tetrahedral coordination at the Ti ions. Given the larger section of the TiO_3 polymer when compared to that of O-bridges, the remaining parts of the surface chains can shrink: this lowers the Ti_{5c}–O_{2c}–Ti_{5c} angles to ∼120°, which is stereochemically more appropriate for twofold coordinated O ions.

Now, we start to study the energetics of thin TiO_2 films peeled off from the surface. The thinnest possible film is made of only one TiO_2 unit for each surface cell, i.e., it is a TiO_2 monolayer. Still, it has the main features of the (001) surface, because it exposes O_{2c} ions connected to Ti ions, even though the latter are now fourfold, instead of fivefold coordinated. The upper and the lower sides of the film are equivalent but rotated by 90°, as a consequence of the pseudo-tetrahedral coordination of the cation. Because the film is no more connected to an underlying bulk phase, its lattice constants can freely relax. As we should expect on the basis of above discussion, the film undergoes a symmetric shrinking (see Fig. 2). This yields a substantial contraction both for the lattice constant (from 3.786 to 3.185 Å), and for the Ti–O–Ti angle (from 150° to 120°), similarly to the (1×4)-reconstructed surface.

These structure changes allow a strong stabilization of the film energy, which passes from 2.09 to 0.65 eV/TiO_2 stoichiometric unit above the bulk phase.

We consider next a 2 ML film, where the surface chains of the top and bottom surfaces run in the same direction. As we already showed in Ref. [7], this film spontaneously undergoes a spectacular transformation, which consists in a gliding of the upper part of the film over the lower part along the direction of the surface chains, and by a simultaneous contraction of the lattice constant along the same direction (see Fig. 2, middle). The final structure is that of lepidocrocite TiO_2, and it is characterized by fully (viz. sixfold) coordinated cations, and by a remarkable stability: only 0.16 eV/TiO_2 above bulk anatase, to be compared with the 0.78 eV of the starting film.

Because the direction of the –Ti_{5c}–O_{2c}– chains rotates by 90° on adding one TiO_2 monolayer, for a 3 ML-film chains at the top and at the bottom surface run in perpendicular directions, as in the 1 ML case. This hampers a anisotropic shrinking of the unit cell, and consequently the attainment of sixfold coordination for Ti cations. Interestingly, however, both the film surfaces assume a canted geometry, which can be interpreted as a (frustrated) attempt to assume a lepidocrocite structure (see Fig. 2, bottom). The converged cell is 3.475×3.475 Å, while cell relaxation lowers the film energy from 0.53 to 0.44 eV/TiO_2.

So far, we have found that (001)-oriented films with an *odd* number of TiO_2 layers have square unit cells, whereas films with an *even* number of TiO_2 layers have a rectangular unit cell, and are characterized by a higher lattice relaxation energy. This trend is maintained at least until $N_{lay} = 6$, as it appears from Table 1 and Fig. 3, where the total energy curves corresponding to films with bulk and relaxed lattice constants are compared. In fact, the solid red curve shows a zig–zag profile, with maxima and minima corresponding to odd and even N_{lay} values, respectively.

For the thickness range here considered, the minimum corresponds to $N_{lay} = 2$, i.e., for the lepidocrocite structure. Thus, optimized structures obtained for $N_{lay} = 4$ and $N_{lay} = 6$ are *not* global minima, since their conversion into two (three) lepidocrocite nanosheets is energetically favored. Another interesting feature of the Fig. 3 graph is that, in contrast to the solid curve, the broken blue curve, which refers to the total energy of the films with bulk lattice constants, displays a monotonously decreasing trend. Thus, the sawtooth profile of the red curve has a completely different nature with respect to that observed, e.g., for the rutile (110) surface, where a different stability of films made of even/odd

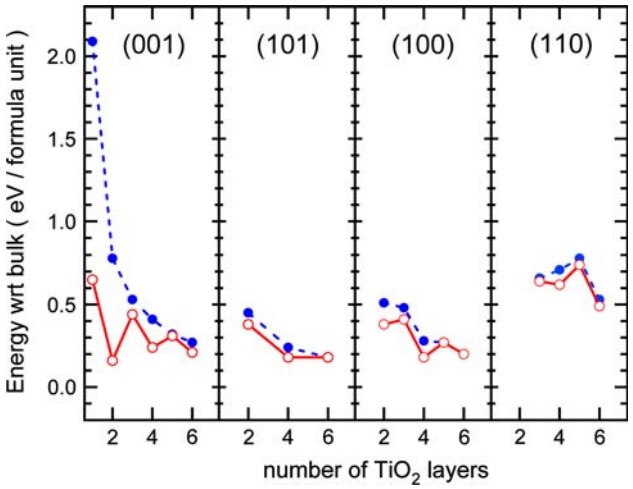

Fig. 3 Total energies of relaxed anatase thin films of 1–6 ML thickness. *Dots* represent calculations where the film constants were constrained to the bulk values, whereas *open circles* refer to totally unconstrained optimizations

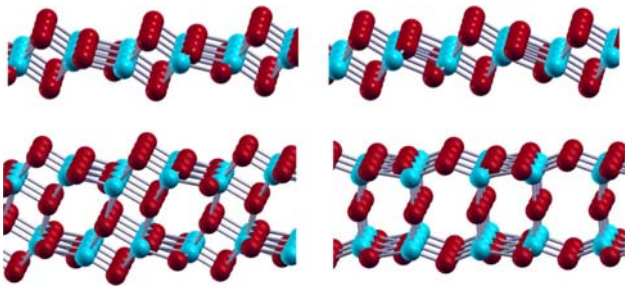

Fig. 4 Relaxed structures of 1 ML (*top*) and 2 ML (*bottom*) (101)-oriented films. Structures on the *left* (*right*) are those obtained with bulk (optimized) constants

number of layers is found even without relaxing the film lattice constants [36].

(101)-oriented films. The (101) surface has a centered rectangular cell, and it can be viewed as a stack of double layers of TiO_2, separated by regions of relatively low density. The (101) surface exposes fivefold and sixfold coordinated cations, as well as twofold and threefold coordinated anions. At variance to the (001) case, the O_{2c} ions connect Ti_{6c} and Ti_{5c} cations, which allows a more efficient ion relaxation. As a result, the (101) surface is much more stable than the (001) one. Because the film is organized in double layers, it makes sense to consider only films made of an even number of TiO_2 layers. Thus, we start by considering the 2 ML case. In tune with the low energy and chemical inertness of the (101) surface [30,31,37–41], this film is rather stable even when adopting the bulk lattice constants (0.45 eV/TiO_2), while cell optimization has a very limited impact both for structure (Table 2 and Fig. 4) and for energy (0.38 eV/TiO_2). The equilibrium cell size is 3.545×10.495 Å to be compared with the 3.786×10.447 Å bulk one.

Table 2 Structural and energy parameters of TiO_2 films derived from the (101) anatase surface, and consisting of an even number layers $2 \leq N_{lay} \leq 6$

N_{lay}	E_{film}	E_{surf}	a'	b'	E'_{film}
2	0.45	0.36	3.545	10.495	0.38
4	0.24	0.40	3.677	11.887	0.18
6	0.18	0.44	3.741	10.423	0.18

E_{film} (in eV/TiO_2) is the film energy wrt. bulk anatase, while E_{surf} is the surface energy (in J/m^2). Both values are computed by constraining the film constants to those of bulk anatase ($a = 3.786$ Å, $b = 10.447$ Å). E'_{film} is the film energy computed for the a' and b' optimized constants

On the basis of the preceding discussion, we could expect a smooth convergence towards a bulk-like situation when increasing the film thickness. Surprisingly, however, we find that for 4-ML film the energy gain obtained by relaxing the cell is larger than that of the 2-ML film (from 0.28 to 0.18 eV/TiO_2). This is due to an unexpected rearrangement of the film, which gives rise to the peculiar structure shown in Fig. 4, that we call "pentacoordinated nanosheet" because all the cations are fivefold coordinated, while the central O ions are converted from threefold to twofold coordinated. We speculate that the driving force of the transformation is the lowering of the O coordination number, since in coordination chemistry the threefold coordination is rather unfavored for oxygen. Remarkably, this nanosheet is *stretched*, rather than *shrinked*, as the lepidocrocite nanosheet: the cell size, in fact, passes from 3.786×10.447 Å to 3.677×11.887 Å. No major restructuring occurs for a 6 ML film (Table 3). The energy of the film with the bulk constants (+0.18 eV/TiO_2) is not appreciably changed by optimizing the lattice constants, and it is equal to that computed for the optimized 4-ML film.

(100)-oriented films. The (100) surface is only slightly less stable than the (101) one. In fact, it contains the same structural elements, but they are differently arranged. As a consequence, films can be built with both an even and an odd number of ML, except for the 1 ML film, which is not complete. The similarity of the (101) and (100) surfaces, coupled to the assumption of no symmetry in the lattice optimization procedure, has the interesting consequence that a 2-ML film is transformed into a 2-ML (101) film, whereas a 4-ML film is converted into the "pentacoordinated" nanosheet which was obtained by optimizing the constants of the 4-ML (101) film.

Because 3-ML (101) films are not possible, the 3-ML (100) film does not undergo a major restructuring, and it turns out to be less stable of both the 2-ML and the 4-ML films.

Notably, this instability of the 3-ML film is not only due to the fact that it cannot be converted into more stable (101)-derived structures, but it seems to be also intrinsic in (100) films made of an odd number of monolayers, as it can be deduced from the total energy curve of the bulk-dimensioned

Table 3 Structural and energy parameters of TiO_2 films derived from the (100) anatase surface, and consisting of a number layers $2 \leq N_{lay} \leq 6$

N_{lay}	E_{film}	E_{surf}	a'	b'	E'_{film}
2	0.51	0.45	3.545	10.495	0.38
3	0.48	0.63	3.639	10.304	0.44
4	0.28	0.49	3.677	11.887	0.18
5	0.27	0.60	3.734	9.582	0.27
6	0.20	0.53	3.753	9.682	0.20

E_{film} (in eV/TiO_2) is the film energy wrt bulk anatase, while E_{surf} is the surface energy (in J/m^2). Both values are computed by constraining the film constants to those of bulk anatase ($a = 3.786$ Å, $b = 9.737$ Å). E'_{film} is the film energy computed for the a' and b' optimized constants

(100) films reported in Fig. 3. In any case, similar to the (101) case, relaxing the film lattice constants for 5- and 6-ML films has practically no effect on the energy.

(110)-oriented films. The (110) surface has a centered rectangular cell, and it is characterized by the presence of Ti_{4c} ions. It should be noted, however, that the coordination of these species strongly deviates from the tetrahedral one, which best suits a moderately ionic compound as TiO_2, and it can be rather described as cis-divacant octahedral. Thus, the (110) surface is the most unstable of those considered so far. To obtain a 2D-film without interruptions we must take at least three monolayers, i.e., one layer of Ti_{6c} ions at the film center and one layer of Ti_{4c} at each surface (see Fig. 5, left). The film relaxation is driven by the necessity of yielding a more stable environment to the Ti_{4c} ions. The resulting structural rearrangement is best described as a rotation in opposite direction of the two Ti_{6c} present in each cell see Fig. 5, right). In this way, the Ti_{4c} ions are converted to Ti_{5c} ions, while half of the O_{2c} ions initially present are converted to O_{3c}. Though the increase of the coordination number of surface oxygens is not usually energetically convenient, this is largely compensated by the modification of the coordination of the Ti ions. Thicker films do not undergo major rearrangements. It is however interesting to note that whereas films composed by an odd number of layers do maintain a rectangular cell, those composed by an even number of layers is slightly distorted to monoclinic symmetry (Table 4).

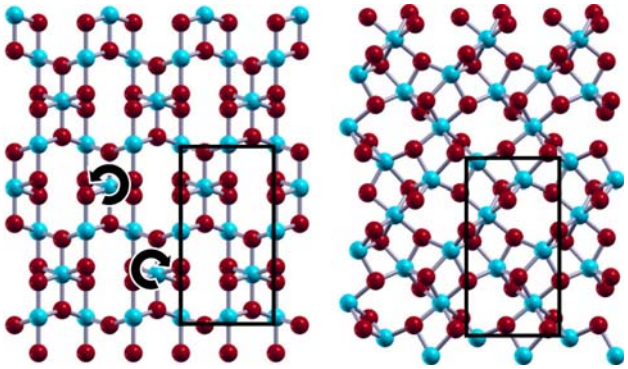

Fig. 5 *Left* top view of a 3-ML (110)-oriented film with the bulk constant. To better show its nature, the *unrelaxed* ionic structure is shown. *Curved arrows* show the rotations undergone by the Ti_{6c} ions upon relaxation. *Right* equilibrium structure of the relaxed film with the optimized constants

Table 4 Structural and energy parameters of TiO_2 films derived from the (110) anatase surface, and consisting of a number layers $3 \leq N_{lay} \leq 6$

N_{lay}	E_{film}	E_{surf}	a'	b'	β'	E'_{film}
3	0.66	1.36	5.195	9.893	90.	0.64
4	0.71	0.85	5.882	9.268	89.27	0.62
5	0.78	1.16	5.473	9.193	90.	0.74
6	0.53	0.95	5.655	9.322	88.65	0.49

E_{film} (in eV/TiO_2) is the film energy wrt bulk anatase, while E_{surf} is the surface energy (in J/m^2). Both values are computed by constraining the film constants to those of bulk anatase ($a = 5.354$ Å, $b = 9.737$ Å, $\beta = 90°$). E'_{film} is the film energy computed for the a', b', and β' optimized constants

4 Conclusion

In conclusion, structural properties of ultrathin anatase layers depend on thickness in a way which which is sensitive to the layer orientation. In particular, we find that: (1) the stability sequence of thinner films does not follow that of related surfaces, (2) notably, (001)-oriented films can compete in stability with (101) and (100) ones of comparable thickness even for 6 ML-thick films, (3) thinner films may exhibit phase transitions, in some cases giving rise to unprecedented structures; (4) stability oscillations are observed when increasing the thickness of films with a given orientation. These oscillations can be already present when the film constants are frozen to the bulk values, or can be induced by the relaxing the constants.

Acknowledgments All the calculations described in this paper have been done with the Quantum Espresso package [42]. Computational resources and assistance were provided by the "Laboratorio Interdipartimentale di Chimica Computazionale" (LICC) at the Department of Chemistry of the University of Padova, and by CINECA (Bologna, Italy). Molecular graphics has been generated by XCrysDen [43].

References

1. Diebold U (2003) Surf Sci Rep 48:53
2. Hagfelt A, Grätzel M (1995) Chem Rev 95:49
3. Hadjivanov KI, Klissurski DG (1996) Chem Soc Rev 25:61
4. Ranade MR, Navrotski A, Zhang HZ, Banfield JF, Elder SH, Zaban A, Borse PH, Kulkarni SK, Doran GS, Whitfield HJ (2002) Proc Natl Acad Sci 99:6481

5. Saponjic Z, Dimitrijvic NM, Tiede DM, Goshe AJ, Zuo X, Chen LX, Barnard AS, Zapol P, Curtiss L, Rajh T (2005) Adv Mater 17:965
6. Bavykin DV, Friedriech JM, Walsh FC (2006) Adv Mater 18:2807
7. Orzali T, Casarin M, Granozzi G, Sambi M, Vittadini A (2006) Phys Rev Lett 97:156101
8. Zhang Y, Giordano L, Pacchioni G, Vittadini A, Sedona F, Finetti P, Granozzi G (2007) Surf Sci (2007) 601:3488
9. Sato H, Ono K, Sasaki T, Yamagishi A (2003) J Phys Chem B 107:9824
10. Sasaki T, Watanabe M, Michiue Y, Komatsu Y, Izumi F, Takenouchi S (1995) Chem Mater 7:1001
11. Unal U, Matsumoto Y, Tanaka N, Kimura Y, Tamoto N (2003) J Phys Chem B 107:12680
12. Zhou Y, Ma R, Ebina Y, Takada K, Sasaki T (2006) Chem Mater 18:1235
13. Osada M, Ebina Y, Fukuda K, Ono K, Takada K, Yamaura K, Takayama-Muromachi E, Sasaki T (2006) Phys Rev B 73:153301
14. Chen Q, Du GH, Zhang S, Peng L-M (2002) Acta Crystallogr B 58:587
15. Wang W, Varghese OK, Paulose M, Grimes CA, Wang Q, Dickey EC (2004) J Mater Res 19:417
16. Enyashin AN, Seifert G (2005) Phys Stat Sol (b) 242:1361
17. Ma R, Fukuda K, Sasaki T, Osada M, Bando Y (2005) J Phys Chem B 109:6210
18. Wen B, Liu C, Liu Y (2005) Chem Lett 34:396
19. Wang F, Jiu J, Pei L, Nakagawa K, Isoda S, Adachi M (2005) Chem Lett 34:1238
20. Zhang S, Chen Q, Peng L-M (2005) Phys Rev B 71:014104
21. Kukovecz A, Hodos N, Horvath E, Radnoczi G, Konia Z, Kiricsi I (2005) J Phys Chem B 109:17781
22. Umek P, Cevc P, Jesih A, Gloter A, Ewels CP, Arcon D (2005) Chem Mater 17:5945
23. Nian J-N, Teng H (2006) J Phys Chem B 110:4193
24. Mao Y, Wong SS (2006) J Am Chem Soc 128:8217
25. Tsai C-C, Teng H (2006) Chem Mater 18:367
26. Wu D, Liu J, Zhao X, Li A, Chen Y, Ming N (2006) Chem Mater (2006) 18:547
27. Riss A, Berger T, Grothe H, Bernardi J, Diwald O, Knozinger (2007) Nano Lett 7:433
28. Morgado E, de Abreu MAS, Moure GT, Marinkovich BA, Jardim PM, Araujo AS (2007) Chem Mater 19:665
29. Alvarez-Ramirez F, Ruiz-Morales Y (2007) Chem Mater 17:2947
30. Lazzeri M, Vittadini A, Selloni A (2001) Phys Rev B 63:155409
31. Lazzeri M, Vittadini A, Selloni A (E) (2002) Phys Rev B 65:119901
32. Vanderbilt D (1990) Phys Rev B 41:7892
33. Perdew JP, Burke K, Ernzerhof M (1996) Phys Rev Lett 77:3865
34. Wentzcovitch RM (1991) Phys Rev B 44:2358
35. Selloni A, Lazzeri M (2001) Phys Rev Lett 87:266105
36. Bredow T, Giordano L, Cinquini F, Pacchioni G (2004) Phys Rev B 70:035419
37. Selloni A, Vittadini A, Grätzel M (1998) Surf Sci 219:402–404
38. Vittadini A, Selloni A, Rotzinger FP, Grätzel M (1998) Phys Rev Lett 81:2954
39. Vittadini A, Selloni A, Rotzinger FP, Grätzel M (2000) J Phys Chem B 104:1300
40. Vittadini A, Selloni A (2002) J Chem Phys 117:353
41. Tilocca A, Selloni A (2004) J Phys Chem B 108:19314
42. Baroni S, dal Corso A, de Gironcoli S, Giannozzi P, Cavazzoni C, Ballabio G, Scandolo S, Chiarotti, G, Focher P, Pasquarello A, Laasonen K, Trave A, Car R, Marzari N, Kokalj A, http://www.pwscf.org/
43. Kokalj A, Comp Mater Sci (2003) 28:155 Code available from http://www.xcrysden.org/